EEET ECOLOGICAL ENGINEERING & ENVIRONMENTAL TECHNOLOGY

Ecological Engineering & Environmental Technology, 25(12), 147–157
https://doi.org/10.12912/27197050/193619
ISSN 2299–8993, License CC-BY 4.0

Received: 2024.09.17
Accepted: 2024.10.15
Published: 2024.11.01

Sustainable Use of Solar Energy to Produce Methanol from Sugar Industry Waste

Soraya Mercedes Pérez[1*]

[1] Department of Natural Resources and Chemical Engineering, Tafila Technical University, P.O. Box 179, Tafila, 66110, Jordan

* Corresponding author's e-mail: soraya@ttu.edu.jo

ABSTRACT

The minimising of environmental pollution is a challenge for Ecuadorian sugar industries. CO_2 from combustion of sugarcane waste (bagasse), needs to be processed immediately after emission. Including ecofriendly energy to replace the use hydrocarbon fuels is other interesting way to reduce the environmental carbonization. Unify these two proposals in the production of a product, is the objective of this innovative work, to the best of our knowledge, it has not been done in Ecuador. CO_2 from burnt sugarcane waste, was captured and reacted with hydrolysed hydrogen to obtain methanol. And, a solar photovoltaic (PV) system was designed to provide clean energy, at the stage of methanol distillation, critical in terms of pollution. Optimum process conditions were found to carry out the distillation in a column 57 plates, flux ratio 1.2 and fed temperature 80 °C. Environmental conditions of geographic region, daily peak sun, technical data about power, voltage, current and material of solar panels and inverter were used in the models proposed by Kayode and Enock for solar system design. Methanol product was purified from 47.5 to 99.92% mol, confirming the effectiveness of the absorption by Monoehtanolamine and distillation as separation methods. Resulted of the energy balance, 650KW is the wattage for powering the overall PV system. 1300 monocrystalline silica solar panels of 500W, were connected to 11 grid string inverters, each one 80 kW, following the optimal design calculated. Our results clearly indicate a novel viability to reduce CO_2 and save hydrocarbon fuel consumption, which is not unlimited resource and main air pollutant.

Keywords: Ecuador, photovoltaic panels, distillation, string grid inverter, energy consumption.

INTRODUCTION

Getting energy from the combustion of hydrocarbon fuels causes serious damage to the nature and health of all living things that populate our planet. And fuels come from hydrocarbons are not unlimited resource. Particularly the sugar cane industries produce large CO_2 emissions. CO_2 emissions come on the one hand, from the combustion of sugar cane waste to obtain steam using boilers, and on the other hand, from the sugars fermentation for producing anhydrous ethanol fuel. The capture and use CO_2 to produce a new product, such as methanol, constitutes an important solution for environmental decarbonization. Methanol is a product widely used in the chemical industry to produce formaldehyde, methyl-tert-butyl ether and acetic acid [Van-Dal et al., 2013]. Methanol also is included a new fuels market as a blend with naphtha for producing dimethyl ether and biodiesel. [Kim et al., 2011; Szima et al., 2018).

The capture and utilization CO_2 from chimney gases by absorption towers, together with the use of solar energy as a replacement for energy from hydrocarbon fuels promising ways of obtaining eco-friendly energy [Tillahodjaev and Mirzaev, 2020]. Installing the Photovoltaic modules (PV) also known as solar panels on residential premises is beneficial residents and also for the state that will save on hydrocarbon fuel (the main air pollutant) that is burned for energy production at thermal power plants [Vladimir et al., 2014]. Photovoltaic power is the cheapest form

of electricity which is generated by interaction of the bundles of radiant energy coming from sun, known as photons, with the semiconductor materials in the PV cells [De Lima et al., 2017). These photons bundles may be reflected, absorbed or transmitted by the PV cell. The absorbed photons generate electricity by transferring their energy to electrons in the atoms of the PV cell made up of a semiconductor material. After receiving the energy from photons, the electrons in the atoms of the semiconductor material become able to escape from their normal positions. After leaving from their positions, they start flowing to become a part of current in the electrical circuit causing the formation of holes in the atomic structure of the cell to allow other electrons to move [Brar et al., 2017]. A built-in electric field in PV cell provides the voltage needed to drive the current through the circuit. The amount of electricity produced by a PV cell depends on its size, its conversion efficiency, and the intensity of the light source. The conversion efficiency of a PV cell may be defined as the proportion of radiant energy converted by a cell into electrical energy, relative to the amount of radiant energy that is striking the PV cell [Reges et al., 2016]. The Photovoltaic cell can produce around 0.5V of electricity, so a few small PV cells are connected and assembled to form a PV modules or panels which absorb the solar radiation and generate usable electrical energy. The solar panels generate direct current electricity (DC) which is converted into alternating current (AC) with the help of an inverter to make it usable to fulfil the household energy needs or to feed the electrical grid. A PV module is the smallest PV component sold commercially and can range in power output from about 10 watts to 500–700 watts. Two or more PV modules can be assembled as a pre-wired, field installable unit to form a PV array [Aoun et al., 2017; Brar et al., 2017]. A general structural diagram of the solar energy system for residence including photovoltaic panels is presented in Figure 1.

Two kinds of solar modules or panels have been widely used: polycrystalline and single or monocrystalline crystal panels. Differing between them in the varieties of silicon semiconductor used for their manufacture. The Polycrystalline modules are most used today, and they composed by several silicon crystal rods which are melted and then poured into a square mold (Figure 2b). The purity of the silicon crystals rods is not as pure as the monocrystalline solar cells; therefore, the resulting solar cells are not identical to each other that seems formed of broken glasses. Its efficiency is lower than monocrystalline panels, ranging between 13% to 16%. The square shape, if it is arranged to form solar panels, will be tight and there will be no wasted empty space like the arrangement of the monocrystalline solar panels. The manufacturing process is easier than monocrystalline; therefore, the price is cheaper [Sugianto, 2020].

The Monocrystalline panels are made by cutting into thin plates of artificially grown silicon crystal (Fig. 2a). This technology produces solar cell pieces that are identical to each other and high performance. So, this type of solar cell becomes more efficient than other of solar cells, achieving efficiency values between 15% to 20%. The high price of pure silicon crystals and the technology used increases the price of this type of solar panel compared to other types of solar panels on the market. The drawback is that this type of solar cell if arranged to form a solar module (solar panel) will leave a lot of empty space because solar cells like this are generally hexagonal or round,

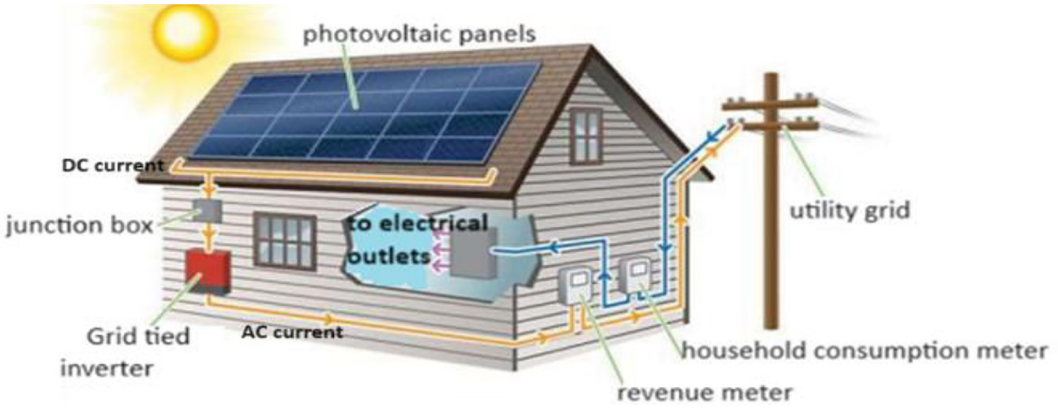

Figure 1. Basic diagram of PV energy system for residence (modified from: Tillahodjaev and Mirzaev, 2020)

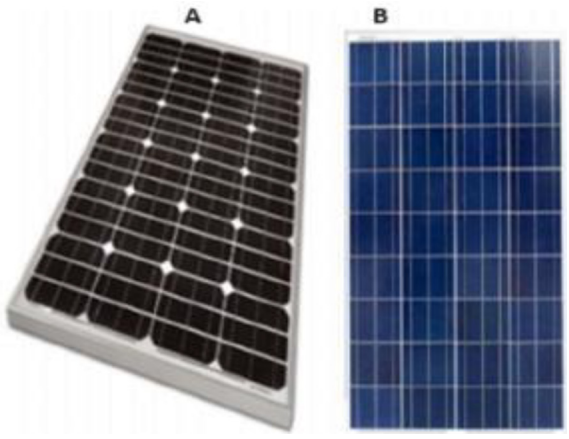

Figure 2. Monocrystalline (a) and polycrystalline, (b) solar panels (modified from Sugianto, 2020)

depending on the shape of the silicon crystal bars [Sugianto, 2020]. The objective of this study is designing a solar system for replace the energy from hydrocarbons fuels used at the stage of methanol distillation.

MATERIALS AND METHODS

In this study the raw material to produce methanol is CO_2 released to the atmosphere by the combustion of sugarcane waste solid (bagasse). The process considers a methanol plant attached to a sugar industry, located at northeastern Ecuador, which processes 1.25 million tons of cane per harvest. The bagasse is combusted to heat the reboiler which produce steam. From this combustion is generated 39521.64 kg.mol/h chimney gas flow rate, whose Orsat analysis reported in Table 3 presented an average content of 8.8% molar CO_2. The chimney gases released of combusted bagasse are washed at 30 °C in scrubbers (wet filters) leaving free of solids particles. Posteriorly, these gases are treated in an absorption tower where CO_2 is absorbed using as solvent monoethanolamine (MEA) aqueous solution 30%W [Meunier et al., 2020; Van-Dal et al., 2013; Li et al., 2016]. The Figure 3 present a flow diagram of CO_2 capture stage.

Solvent enriched in CO_2 leaving of absorption tower is send to regeneration column, previous pressurization and heating to bubble temperature, to recover monoethanolamine and recycle to the absorption column. The CO_2 recovered from the regeneration column top is constituted mainly CO_2 and vapor of water. Water vapor is condensed and separated by flash distillation, achieving purity level CO_2 around 99.8%. Purified gas CO_2 is fed to the methanol plant.

Methanol production

Purified CO_2 is fed to the methanol plant along with the hydrolysed hydrogen following the process recommended by Pérez Fortes et al. [2016]. At first stage of the process, the feed gases (hydrolysed H_2 and purified CO_2) are compressed achieving the reactor feed pressure, using several compression and cooling stages. At second stage the pressurized feed is heated and reacted in the reactor obeying the reactions A and B, obtaining methanol product and water as subproduct.

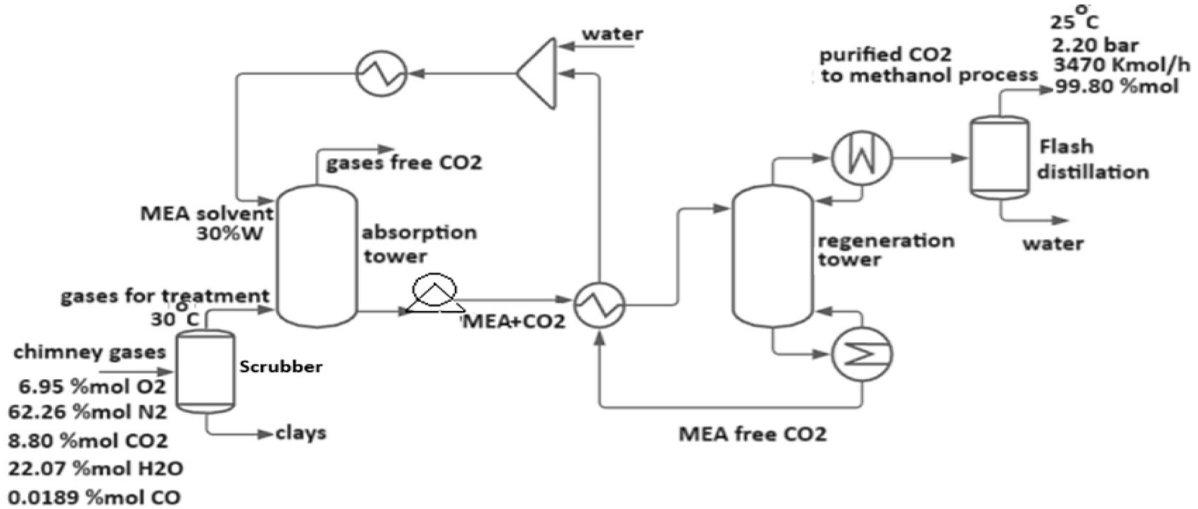

Figure 3. Capture & purification CO_2 of chimney gases from combusted sugarcane bagasse (modified from: Cuezzo et al., 2021)

$$CO_2 + 3H_2 \rightarrow CH_3OH + H_2O \quad (A)$$

$$CO_2 + H_2 \rightarrow CO + H_2O \quad (B)$$

The stream leaving of the reactor is directed to a flash distillation where the mixture methanol-water suffers a first water separation. The condensed of flash distillation is a mix methanol-water with methanol 61.7%W. At third stage, the mixture of methanol 61.7%W is fed a distillation column where will continue the purification of methanol. At third stage, the methanol is separated from water in a distillation column, and this stage will focus the energy study for the design of the solar energy system. The reactor and distillation column conditions are presented in Figure 4.

Energy consumption

To calculate many types of properties of mixtures required in the energy balance, such as molecular weight (M_{mix}), heat capacity (Cp_{mix}) or temperature (T_{mix}), the mixing ruler (eq. 1) is applied considering the ideal nature of the solution methanol-water. Properties of pure compounds (M_i, Cp_i, etc.) have been taken to average temperature T, being $T = (T_o + T_f)/2$, between the temperatures of fluid enters T_o and leaves T_f of the heat exchanger. These values have been used for application of the mixing ruler. Examples of the conversion of mass fraction values (X) to molar fraction (x) are expressed by the Equations 2 and 3:

$$M_{mix} = \sum x_i M_i,\ Cp_{mix} = \sum x_i Cp_i,\ T_{mix} = \sum x_i T_i \quad (1)$$

$$x_{methanol} = (X_{methanol}/M_{methanol})/ [(X_{methanol}/M_{methanol}) + (X_{water}/M_{water})] \quad (2)$$

$$x_{water} = (X_{water}/M_{water})/ [(X_{methanol}/M_{methanol}) + (X_{water}/M_{water})] \quad (3)$$

$$Load_{actual} = (Q_{exchanger\ A}) = m \cdot (T_f - T_o) \cdot Cp_{mix} \quad (4)$$

The energy consumption ($Load_{actual}$ or Q) is computed through an energy balance around each exchanger equipment by equation 4, using the inlet (T_o) and outlet streams temperatures (T_f), mass flow rate (m) and heat capacity (C_p). For the compressors and pumps, the technical data give us the load actual per device.

Design of energy system

Solar panels of monocrystal silica with wattage values around 500 W were used in this design following recommendations by Ed [2019] for grid-connected solar energy. The technical sheet presents the specifications for different parameters of the solar panels and inverter (Table 1).

To calculate the number of the solar panels Np using equation 6, previously is necessary calculate daily array size in Watts by equation 5 proposed by Kayode and Enock [2022]. Where, PW value is the total daily consumption power obtained from the summation of monitored Load actual (Table 5).

The system's efficiency derate factor or overall efficiency factor E = 0.66 has resulted of the multiplication of security factors due to temperature losses (0.88), inverter efficiency (0.96) and general system derate factor (0.774) [Ed, 2019]. Daily peak sun hours (PSH) are in function of the geographic region. PSH value represents the solar insolation hours per day which reaches at 1000 W/m^2, being 4.5 for northeastern zone of Ecuador [https://info.undp.org/docs/pdc/Documents].

$$Daily\ array\ size = PW/[(PSH) \times E] \quad (5)$$

Table 1. Data of technical sheet

Solar panel		Inverter	
STC Power (Pmp)	500 W	Nominal voltage	600 V
Maximum power voltage (Vmp)	53.94 V	MPPT voltage range	200V–1000 V
Maximum power current (Imp)	9.27 A	N° of MPP trackers	7
Open circuit voltage (VOC)	65.92 V	N° PV strings/MPP trackers	2
Short-circuit current (Isc)	9.77 A	Power	80 kW
Temperature coefficents	TkVoc -0.308% °C	Max.input current/MPP tracker	26 A
	TkVmp -0.42% °C	Max.short circuit current/ MPPtracker	32 A
Material	Mono crystal silica panel	Type	String inverter

Note: https://powersyncenergy.com

$$Np = Daily\ array\ size\ (Watt)/(Watt\ of\ solar\ panel) \quad (6)$$

Inverter sizing

The following step is determining the inverter sizing. The selection of the inverter power should consider direct current (*DC*) voltage produced from panels remains within the voltage range of the inverter. The maximum and minimum number of panels or panels in series that can be connected to the inverter are calculated for equations 7 and 8. These equations are in function of corrected voltage VOC_{max} and Vmp_{min} (Eq. 9 and 10), where the ambient temperature is a critical factor [Ed, 2019; Osterberg, 2013]. VOC_{max} is maximum module voltage corrected for the site lowest expected ambient temperature, Vmp_{min} is minimum module voltage expected at site high temperature. T_{min} and T_{max} are the minimum and maximum ambient temperature achieved at location where the inverter is installed, fluctuating for northeastern zone of Ecuador, values between 23°C and 38°C [https://www.researchgate.net/publication/338843581_Mapa_Solar_del_Ecuador_2019]. T_{STC} is the STC temperature at 25°C [STC is an industry-wide standard to indicate the performance of PV modules and specifies a cell temperature of 25°C and an irradiance of 1000 W/m^2 with an air mass 1.5 (AM1. 5) spectrum]. Tk_{VOC} and Tk_{Vmp} values are maximum and minimum temperature coefficients and T_{add} is adder temperature for estimating solar module cell. Table 2 presents recommended values for T_{add}:

$$Panels\ or\ series\ panels_{max} = max.voltage\ MPPT\ of\ inverter/VOC_{max} \quad (7)$$

$$Panels\ or\ series\ panels_{min} = min.voltage\ MPPT\ of\ inverter/Vpm_{min} \quad (8)$$

$$VOC_{max} = VOC \cdot [1 + (T_{min} - T_{STC}) \cdot TkVOC] \quad (9)$$

$$Vmp_{min} = Vmp \cdot [1 + ((T_{add} + T_{max} - T_{STC}) \cdot TkVmp)] \quad (10)$$

Table 2. Adder temperature for estimating solar system

Location	Adder temperature
Poler or ground	25°C
Tilted racks on roof	30°C
Roof mount	35°C

Note: Ed, 2019.

Appling the upper equations are obtained VOC_{max} and Vpm_{min} for this study. The maximum and minimum panels or series panels would be wired to inverter are calculated following:

$$VOC_{max} = 65.92\ V \cdot [1 + (23\ °C - 25\ °C) \cdot (-0.308/100)\ °C] = 66.32\ V$$

$$Vpm_{min} = 53.94\ V \cdot [1 + (30\ °C + 38\ °C - 25°C) \cdot (-0.42/100)\ °C] = 44.198\ V$$

$$Panels\ or\ series\ panels_{max} = 1000/66.32 = 15\ panels$$

$$Panels\ or\ series\ panels_{min} = 200/44.198 = 5\ panels$$

Other quickly method to estimate minimum and maximum number of panels is by division of the minimum and maximum values of the operating voltage range of the inverter per open voltage circuit (*VOC*) (Eq. 11 and 12). Data of the solar panel were taken from technical sheet (Calculating Solar PV String Size - A Step-By-Step Guide - SolarDesignGuide)

$$Panels\ or\ panels\ series_{max}: max.voltage\ MPPT/VOC\ panel \quad (11)$$

$$\text{Panels or panels series}_{min}: \text{min.voltage MPPT /VOC panel} \quad (12)$$

$$Panels\ or\ panels\ series_{max} = 1000/65.92 = 15.16\ panels$$

$$Panels\ or\ panels\ series_{min} = 200/44.198 = 3\ panels$$

For panels in series, the voltage (V_{serie}) and current (A_{serie}) are calculated obeying the series circuit's law (Eq. 13 & 14), where V_i and A_i are the voltage and current for each panel respectively. For inverters or panels connected in parallel, the voltage ($V_{parallel\ system}$) and current ($A_{parallel\ system}$) are calculated by equations 15 & 16. The power of a inverters system connected in parallel is calculated by equation 17 where P_i is the power of each inverter and N_i the number of inverters.

$$V_{serie} = \sum Vi \quad (13)$$

$$A_{serie} = A_i \quad (14)$$

$$V_{parallel\ s} = Vi \quad (15)$$

$$A_{parallel} = \sum A_i \quad (16)$$

$$Power\ inverter\ system = P_i \cdot N_i \quad (17)$$

RESULTS AND DISCUSSION

The process of methanol production

Results of Orsat analysis of the chimney gases composition released from burned bagasse, are presented in Table 3.

The Orsat results reported in Table 3 indicate levels CO_2 8.8% molar, in accordance with other studies about chimney gases released from direct combustion of sugarcane bagasse, where CO_2 into range 7–10% molar [Shukla and Kumar, 2018]. Although this CO_2 level represent a significant amount of CO_2 present as pollutant air of environmental point of view, other significant pollutant emitted by bagasse-fired boilers is particulate matter, caused by the turbulent movement of combustion gases. Bagasse generally contains 50% fiber, 48% moisture and 2% sugar which couldn't be extracted [Chauhan et al., 2011] even if the composition of combustion gases depends on the nature and amount of cellulose content of the combusted sugarcane. The high energy emitted from combusted bagasse is used in our process, for heating water, producing steam of high quality as also was experimented by Sotiris [2020].

The results reported after absorption and flash distillation (Fig. 3), revealed improving of the purification of CO_2 fed from 8.8 to 99.8% mol, indicating excellent efficiency in the separation processes and correct selection of solvent for absorption (Monoethanolamine; MEA). The high CO_2 absorption in Monoethanolamine is due to the formation of carbamate according to the zwitterion mechanism, followed by the hydration of CO_2 to form HCO_3^-/CO_3^{2-}, and accompanied by the hydrolysis of carbamate [Lv et al., 2015]. This mechanism convert MEA in a suitable solvent for the absorption operation, complemented by flash distillation to eliminate traces of steam. Similar levels of purity of CO_2 were observed by Cuezzo et al. [2021] for carbon dioxide absorbed from chimney gas using MEA. Purified CO_2 is reacted with hydrolysed hydrogen to produce methanol (Figure 4). For best synthesis of methanol and separation from water, the method applied consider the stages of compression with intercooling, reaction, and distillation at ambient pressure. The compression incorporates abrupt reduction of pressure, innovation of this work, which improving similar method used by Perez Fortes et al. [2016].

Table 3. Orsat analysis of the chimney gases of bagasse combustion

N2	H2O	CO2	CO	O2
62.26%*	22.07%	8.8%	0.0189%	6.95%

Note: *Mol percentage.

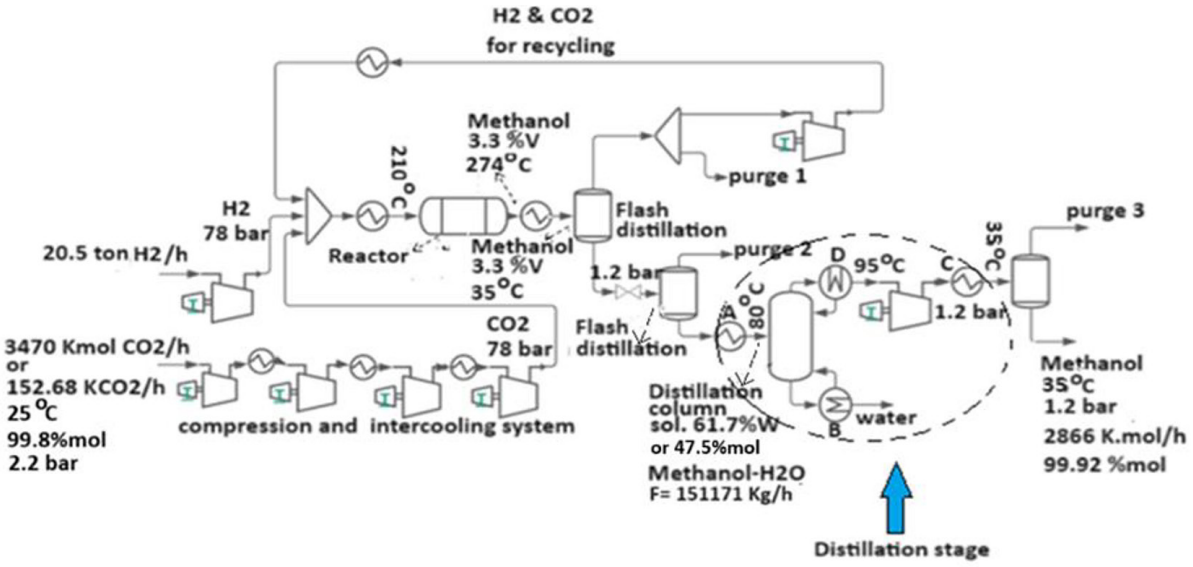

Fig. 4. Plant of methanol production (modified from Cuezzo et al., 2021)

The fed, F = 151171 Kg/h enters to the distillation column (Fig. 4; distillation stage), coming from the flash distillation. Fed stream *F* is a mixture, consisting mainly of methanol and water. Analysis of fed enters to distillation column, reveal compositions of 61.7% $W_{methanol}$ and 38.3%W_{H2O}. Presenting the fed characteristics of ideal solution (sol. ethanol-water) due to its complete solubility between both components, which allow estimate the properties of mixture applying mixing ruler equation (eq.1), specific for ideal solutions. This behaviour occurs because methanol and water have similar properties because both have hydroxyl groups that can form hydrogen bonds. Methanol forms a hydrogen bond with water and is therefore miscible (soluble in all proportions) in this solvent [Huertas et al., 2015]. At the stage of methanol distillation by column (Fig. 4), the purity of methanol improved from 47.5 to 99.2%mol, indicating that conditions of reflux (1.20), feed (80 °C), condenser pressure (1 atm) and number of plates (57 trays) found for our process were optimal.

Energy consumption at distillation stage

The consumption energy analysis required for the design of the energy solar system, will focus on the stage of methanol distillation due to it requires a high demand of energy used for the heat exchangers systems (Fig. 4; distillation stage).

Usually, the load actual consumption, expressed in Watts, is calculated with the wattage data taken from the technical sheets of electrical equipment. But an interesting contribution of this work is the conversion of the kinematic energy of exchangers currents into calorific energy and posteriorly load actual consumption, through heat balances (Equations 1 & 4). So, the following example illustrates the calculation of load actual for the heat exchanger *A*. The values of load actual are multiplied per the working hours/day to obtain daily consumption at kW·h/day; whose summation expresses total daily consumption presented in Table 4.

$$Cp_{mix} = 0.48\cdot(2.84\ kJ/kg°C) +$$
$$+ 0.52\cdot(4.2\ kJ/kg°C) = 3.54\ kJ/kg°C$$

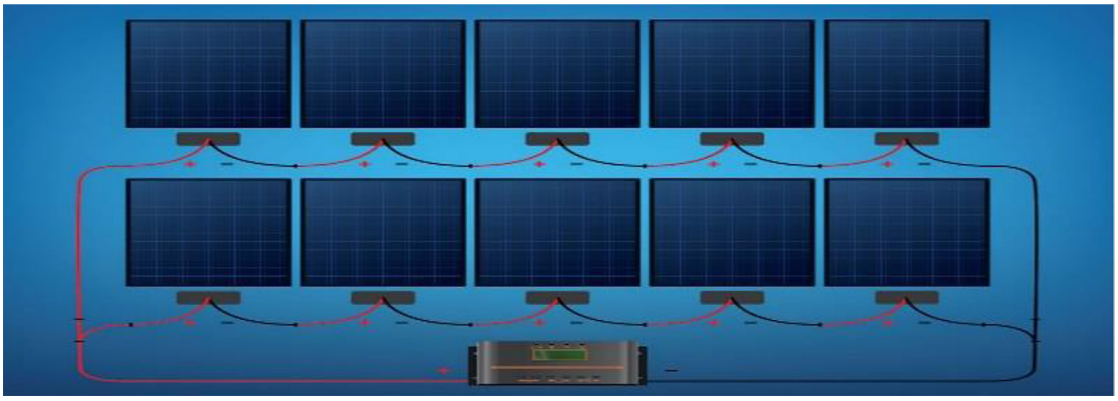

Fig. 5. Example of two chains of panels in series, which are connected parallelly to a string grid inverter. Each chain is constituted of 5 panels (taken from: www.energy2Store.hr/en/)

Table 4. Total daily consumption power (PW) from results of energy consumption at the stage of column distillation process

Device	Quantity	$Load_{actual}$ (kW)	$Load_{Total}$ (kW)	$Operating_{time}$ (h/day)	W·h/day
Compressors	3	75	225	8	225·8 = 1800
Centrifuge pump	4	2.24	9	8	72
Heat exchanger A	1	4.1	4.1	8	32.8
Heat exchanger B	1	0.34	0.34	8	2.72
Heat exchanger C	1	2.8	2.8	8	22.4
Condenser D	1	0.36	0.36	8	2.88
Total daily consumption power	PW = ∑1932.8 kW·h/day Daily array size (required consumption) = 650 kW				

Note: kW = kilowatt.

$$Load_{actual} = 92434 \text{ kh/h} \cdot \cdot(80–35)°C\ (3.54\ kJ/kg°C) \cdot 3600\ s/h = 4.1\ kW$$

Comparing total daily consumption at distillation stage, 1932.8 kW·h/day, with other energy studies for sugar industries analysed by Cuezzo et al. [2019], it would represent approximately 25% of total consumption energy of the process of synthesis of methanol. Energy consumption that could be saved from hydrocarbon fuels combustion, following the proposal of this study, which considers including a photovoltaic solar system for this distillation stage.

Design a solar energy system

Daily array size and number of solar panels

Minimization of CO_2 pollution was achieved in a first stage by obtention of methanol from CO_2 released during the combustion of bagasse. Continuing with the objective of reducing environmental carbonization, the energy from fossil fuels required at distillation stage of methanol, is replaced by solar energy from the photovoltaic system designed for our process. Distillation was the selected stage because is one of the most critical in terms of environmental pollution. So, we choose photovoltaic solar panels because it is the technology which is heading the solar integration to industry in a big part of the world. Monocrystalline silica solar panels with wattage values around 500 W were considered, following recommendations discussed by Ed [2019] for grid-connected solar energy and panels of high power available in the market. Panels of monocrystalline silica were selected because its property of magnify the inlet micro power by the relatively constant production of electricity, by mean of semiconducting materials with a photovoltaic effect, and the possibility to use the stored electrical energy even in absence of sunlight [Quijera et al., 2011; Li et al., 2005]. Additionally, they have a slightly higher efficiency to convert solar energy into electrical energy, 20% more than polycrystalline panels, meaning they can produce more energy per unit area. The results of Equations 5 and 6 used by Kayode & Enock [2022] to determine the daily array size and number of solar panels (Np) are shown in Table 5 and illustrated following:

$$\text{Daily array size(required consumption)} = \\ = (1932.8\ kW \cdot h/day)/[(4.5\ h/day) \cdot 0.66)] = \\ = 650 \cdot 10^3\ W = 650\ kW\ Np = (650 \cdot 10^3\ W)/ \\ (500\ W/panel) = 1300\ \text{solar panels}$$

An array with a series string of 1300 modules can produce 650 kW, being able to supply the required energy.

Size of the inverter

Including an inverter in the design of a solar system is necessary to convert the direct current

Table 5. Results of voltage, current and power for different proposal arrangements for a design of solar energy system

Proposal	Series wired parallelly per inverter	Panels per series	Voltage per serie (eq.13)	Current per Serie	Voltage per inverter	Current per inverter (eq.16)	Wattage per inverter(eq.17)	Panels per inverter	Number of inverters	Total wattage of inverters wired parallel	Observation
1	15	15	65.92·15 = 989 V	9.27 A	989 V	15·9.27 = 139.1 A	989V·139.1A = 137.56 kW	15·15 = 225	1300/225 = 6	-	** Non-viable
2	15	10	65.92·10 = 659.2 V	9.27 A	659.2 V	15·9.27 = 139.1A	659.2V·139.1A = 91.69 kW	15·10 = 150	1300/150 = 9	-	** Non-viable
3	15	9	65.92·9 = 597.28 V	9.27 A	597.28 V	15·9.27 = 139.1A	597.3V·139.1A = 82.52 kW	15·9 = 135	1300/135 = 10	-	** Non-viable
4	15	8	65.92·8 = 527.2 V	9.27 A	527.2 V	15·9.27 = 139.1A	527.2V·139.1A = 73.33 kW	15·8 = 120	1300/120 = 11	80 kW·11 = 880 kW	+ Viable
Comparation between values estimated and calculated of maximum and minimum number of panels or panels in series wired to inverter											
Max. series wired inverter	15 →	15.2 →	Results using corrected equations 7 & 8 40.52V VOC_{max} 23.34V Vmp_{min}	→ %Margin of difference = 100·(15.2–15)/15 = 0.8%							
Min. series wired inverter	5 →	3 →	Results estimated using equations 11 & 12	→ %Margin of difference = 100·(3–5)/5 = -40%							
Required wattage and panels for the design of solar system: 650 kW and 1300 panels, technical data: Solar panels 500W; VOC = 65.92 V; 9.27A; String inverter: 80 kW, MPPT voltage range: 200–1000 V											

Note: +viable because it is within range of the nominal voltage, power and current of the inverter; ** non-viable because exceeding the nominal range of voltage or power of the inverter.

electricity (DC) produced by the solar array to alternating current (AC) electricity. Result of Equation 5 shows a high daily array size 650 kW, which should be covered. For this reason, string grid inverters 80 kW of high power available on the market, were used to cover more easily required wattage in this study (650 kW). The use of grid inverter in accordance with Sunitha et al. [2017], was also taken account for design of highly efficient solar system. Table 5 shows different arrangements of panels series could connect to inverter for cover the required consumption (650 kW). So, the versatility and viability to connect this type of inverters in parallel to build system current, will allow to wire the 1300 solar panels required to cover the daily array size, by connecting chains of panels in series and parallel. Taking account that these chains obey series and parallel's laws, working as same way (Equations 13, 14, 15 and 16).

So, if there is a problem with the connection of one of the panels in the series, the entire circuit fails. While a faulty panel or a loose wire in a parallel circuit would not affect the production of the rest of the solar panels. The results of Table 5 reveal maximum 15 and minimum 5 number of panels or panels series would be wired to the inverter. Corrected values of 66.32 V VOC_{max}(maximum module voltage corrected for the site lowest expected ambient temperature) and 44.198 V module Vmp_{min} (minimum module voltage expected at the site high temperature) were used to determine the limit of solar panels. These values were corrected to environmental temperature of northeastern zone of Ecuador (max 38 °C & min 23 °C) and T_{adder} value 30°C was used to determine Vmp_{min}, which is recommended for tilted rack on roof [Osterberg, 2013]. The results of Table 5 shows clearly that the arrangement # 4 (73.33 kW), is the most viable arrangement, because they do not exceed 80 kW of the inverter. For increasing the wattage of the system and cover the required 650 kW, parallel connections of the inverters were used. So, following the optimum results of arrangement #4, 11 inverters 80 kW wired in parallel should be required. The distribution should be: 15 solar panels chains connected parallelly to an inverter, and each chain is constituted 8 solar panels connected in series. Figure 5 presents an example of two chains of solar panels in series wired in parallel with a string inverter.

The estimated values of panels in series would be connected to inverter, obtained by equations 11 and 12, differ -8% and 40% of maximum and minimum number of panels calculated by corrected voltage equations 7 & 8 (VOC_{max} and Vmp_{min}). This corrected equation is more accuracy because the minimum and maximum levels of ambient temperature is a factor affects the inverter. A high temperature, which results in high solar cells temperature, can result in array voltage loss. But while low environmental temperatures can result in increased array voltage production. Failure to achieve the minimum voltage due to high temperatures results in inverter shut down. Likewise, exceeding the maximum voltage due to low temperatures also results in the inverter going offline, and produce damage in the inverter [Osterberg, 2013].

Although in this work, the photovoltaic design was done for the methanol distillation stage, which demands high energy consumption, the same analysis may be applied to all processes in plant, with the consequent readjustment of the wattage of the solar system design.

CONCLUSIONS

This study reduces 25% of the required energy from fossil fuels, which is necessary to carry out the distillation stage of methanol, by implementation of photovoltaic system (PV). The process conditions found in this study were optimum. At the stage of capture and absorption CO_2, the best solvent and concentration identified was Monoethanolamine (MEA) at 30%. So, CO_2 stream fed to the methanol plant, improved its purity from 8.8% mol to 99.8% mol. At the methanol plant, the innovation of the method by abrupt compressions at 2.2 bar, in the compression and intercooling system, was successful, facilitating cooling of the feed to the distillation column. High purity of distilled methanol (99.92% mol) was achieved in a distillation column of 57 trays, 80 °C feed temperature, 1 amt condenser pressure and 1.2 reflux ratio.

Regarding the photovoltaic design, the results of this analysis revealed that to cover 650 kW required at the distillation stage, 1300 solar panels of 500 W each one, and monocrystalline silica material are needed. From analysed arrangements, all of them, the best one corresponds for 11 grid string inverters, each one 80 kW, connected

between them in parallel. Fifteen strings of panels in series are connected each inverter. Each string of panels is constituted 8 panels. With this design, the required consumption 650 kW would be covered, without exceeding the nominal voltage of the inverter.

The results showed that the difference of error percentage between the estimated and calculated values of the maximum and minimum number of strings that can be connected to the inverter, are 8% and 40% respectively. It indicates the notable effect of temperature, which should be taking account on the calculation of the panels's numbers, especially in tropical climates such as Ecuador.

Although processed CO_2 represents almost the entire amount of this compound present in the emission gases of burnt bagasse, it only corresponds 5% mixture of combustion gases, which is not enough to slow down environmental pollution. However, this novel study revealed an integral method, processing CO_2 and inclusion solar energy, for reducing environmental pollution, that could be carried out with the other components of the flue gas. The application of work is encouraging because opens a new perspective for the integration of clean energy; and the implementation of processing policies for combustion gases emitted in the distinct stages of production. Becoming a challenge in the field of chemical engineering a way of energy saving and environmental conservation.

This work does not contemplate the study of batteries for keeping solar energy produced by the photovoltaic system, presenting difficulties during recharging these devices. The analysis of the design of these devices, should be the subject of study for future research.

REFERENCES

1. Andreado S. 2020. Modelling of bagasse combustion. www.researchgate.net/publication/340315422_Modelling_of_bagasse_combustion
2. Aoun N., Bouchouicha K., Chenni R. 2017. Performance Evaluation of a Mono-Crystalline Photovoltaic Module Under Different Weather and Sky Conditions. International Journal of Renewable Energy Research, 7(1), 292–297.
3. Brar Singh M., Kumar1 R., Sarita, Sushil K.2017. Conversion of Solar Energy into Electrical Energy Using Photovoltaic Technology: A Review. International Archive of Applied Sciences and Technology, 8(4), 14–18.
4. Chauhan M.K., Varun C.S., Suneel K.S. 2011. Life cycle assessment of sugar industry: A review. Renewable and Sustainable Energy Reviews, 15, 3445–3453.
5. Cuezzo A., Araujo P., Mele F. 2021. Simulacion de un proceso de fabricacion de methanol a partir de fuentes renovables. Simposio Argentino de Informática Industrial e Investigación Operativa (50JAIIO – SIIIO-ISSN: 2618-3277), 20–31.
6. De Lima L.C., De Araujo Ferreira L., De Lima Morais F.H. 2017. Performance Analysis of a Grid Connected Photovoltaic System in Northeastern Brazil, Energy for Sustainable Development, 37, 79–85.
7. Ed F. 2019. Calculation of a grid connected solar energy system. Cooperative extension of University of Arizona, 1–8.
8. https://info.undp.org/docs/pdc/Documents. Last visit: 04-09-2024
9. https://www.researchgate.net/publication/338843581_Mapa_Solar_del_Ecuador_2019. Last visit: 04-09-2024
10. Kayode M., Enock A. 2022. Design of a PV system. Global Scientific Journal, 10(6), 1233-1243.
11. Kim J., Henao C.A., Johnson T.A., Dedrick D.E., Miller J.E., Stechel E.B. 2011. Methanol production from CO_2 using solar-thermal energy: process development and techno-economic analysis. Energy Environ Sci, 4, 3122–3132.
12. Li Danny H.W., Cheung Gary H.W., Lam Joseph C. 2005. Analysis of The Operational Performance and Efficiency Characteristic for Photovoltaic System in Hong Kong. Energy Conversion and Management, 46(7–8), 1107–1118.
13. Li B.H., Zhang N., Smith R. 2016. Simulation and analysis of CO_2 capture process with aqueous monoethanolamine solution. Applied Energy, 161, 707–717.
14. Lv B., Guo B., Zhou Z., Jing G. 2015. Mechanisms of CO_2 Capture into Monoethanolamine Solution with Different CO_2 Loading during the Absorption/Desorption Processes. Environmental Science & Technology, 49(17), 10728–10735. https://doi.org/10.1021/acs.est.5b02356
15. Meunier N., Chauvy R., Mouhoubi S., Thomas D., De Weireld G. 2020. Alternative production of methanol from industrial CO_2. Renewable energy, 146, 1192–1203.
16. Osterberg K. 2016. Selecting appropriate PV array string sizes. Home Power Magazine, 173, 16–18. Retrieved from: https://www.homepower.com/articles/solar-electricity/ design-installation/methods-selecting-appropriate-pv-array-string-sizes.
17. Pérez-Fortes M., Schöneberger J.C., Boulamanti A., Tzimas E. 2016. Methanol synthesis using captured CO_2 as raw material: Techno-economic and environmental

assessment. Applied Energy, 161, 718–732.

18. Quijera J.A., González M., Labidi J. 2011. Usage of Solar energy in an industrial process. Chemical Engineering Transactions, 25, 875–880. DOI: 10.3303/CET1125146
19. Reges J.P., Braga E.J., Dos L.C., Mazza S., De Alexandria A.R. 2017. Inserting photovoltaic solar energy to an automated irrigation system. International Journal of Computer Applications, 134(10), 90–98.
20. Saly V., Vary M., Packa J., Firicky E., Perny M., Kubica J. 2014. Performance And Testing of a Small Roof Photovoltaic System. Journal Of Electrical Engineering, 65(7s), 15–19.
21. Shukla A., Kumar S. 2018. Comparative study of sugarcane bagasse gasification and direct combustions. Jr. of Industrial Pollution Control, 34(2), 2063–2074. www.icontrolpollution.com
22. Sugianto P. 2020. Comparative Analysis of Solar Cell Efficiency between Monocrystalline and Polycrystalline. Jurnal Penelitian, 7(2), 92–100. http://dx.doi.org/10.31963/intek.v7i2.2625
23. Sunitha K.A., Prem Kumar G., Nidhi Priya, Jatin Verma. 2017. Design of Highly Efficient MPPT Solar Inverter. MATEC Web of Conferences, 108, 14004. DOI:10.1051/matecconf/201710814004
24. Szima S., Cormos C.C. 2018. Improving methanol synthesis from carbon-free H_2 and captured CO_2: A techno-economic and environmental evaluation. Journal of CO_2 Utilization, 24, 555–563.
25. Tillahodjaev R.R., Mirzaev A.A. 2020. Calculation of the solar energy system. International Journal of Innovations in Engineering Research and Technology, 54–57.
26. Van-Dal É.S., Bouallou C. 2013. Design and simulation of a methanol production plant from CO_2 hydrogenation. Journal of Cleaner Production, 57, 38–45.